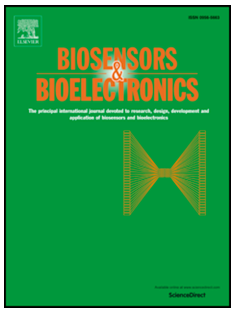

Label-free probes using DNA-templated silver nanoclusters as versatile reporters

Yahui Guo, Xinyue Pan, Wenya Zhang, Zhigang Hu, Ka-Wang Wong, Zhike He, Hung-Wing Li

PII: S0956-5663(19)31005-X

DOI: https://doi.org/10.1016/j.bios.2019.111926

Reference: BIOS 111926

To appear in: *Biosensors and Bioelectronics*

Received Date: 28 September 2019

Revised Date: 17 November 2019

Accepted Date: 25 November 2019

Please cite this article as: Guo, Y., Pan, X., Zhang, W., Hu, Z., Wong, K.-W., He, Z., Li, H.-W., Label-free probes using DNA-templated silver nanoclusters as versatile reporters, *Biosensors and Bioelectronics* (2019), doi: https://doi.org/10.1016/j.bios.2019.111926.

Label-free probes using DNA-templated silver nanoclusters as versatile reporters

Yahui Guo,[ab] Xinyue Pan,[a] Wenya Zhang,[a] Zhigang Hu,[c] Ka-Wang Wong,[b] Zhike He[d] and Hung-Wing Li*[b]

[a] *State Key Laboratory of Food Science and Technology, Jiangnan University, Wuxi 214122, China*

[b] *Department of Chemistry, Hong Kong Baptist University, Kowloon Tong, Hong Kong, China*

[c] *Wuxi Children's Hospital, Wuxi People's Hospital affiliated to Nanjing Medical University, Wuxi, China*

[d] *College of Chemistry and Molecular Sciences, Wuhan University, Wuhan 430072, China*

Correspondent: hwli@hkbu.edu.hk (HW. Li)

Abstract

DNA-templated silver nanoclusters (DNA-AgNCs) have demonstrated pervasive applications in analytical chemistry recently. As a way of signal output in DNA-based detection methods, DNA-AgNCs have prominent advantages: first, the recognition and synthesizing sequences are naturally integrated in one DNA probe without any chemical modification or connection; second, the emissive wavelength of DNA-AgNCs can be adjusted in a wide range by employing different sequences; third, DNA-AgNCs can be utilized for producing not only fluorescence, also electrochemiluminescence and electrochemical signals. Besides, they also show potential applications for cell imaging, and are considered to be one of the most ideal nanomaterials for in-vivo imaging due to their ultra-small particle size. In this review, a brief and comprehensive introduction of DNA-AgNCs is firstly given, then label-free probes using DNA-AgNCs are classified and summarized, lastly concluding perspectives are provided on the defects and application potentials.

Keywords: DNA silver nanoclusters; label free; biosensor; fluorescence; electrochemiluminescence.

Content

1 Introduction

Noble metal nanoclusters with sizes comparable to the electronic *Fermi* wavelength consist of a few to several hundreds of metal atoms (Service 1996), exhibit molecular-scale discrete energy levels and unique characteristics which are different from nanoparticles. The unique physical and chemical properties endow the nanoclusters good performances including excellent dispersibility, good stability, biocompatibility (Zhang et al. 2014), high catalytical activity (Yang et al. 2018), photoluminescence (Grandjean et al. 2018) and electroluminescence (Gonzalez et al. 2004), which have attracted substantial research in recent years (Cao et al. 2018; Yao et al. 2018). Among the nanoclusters, DNA-templated silver nanoclusters (DNA-AgNCs) have attracted special attentions as a class of fluorophores and have been employed in disease diagnosis, environmental monitoring, food hazards detection, cell imaging etc. (Liu 2014).

The specific affinity of silver ions towards cytosine makes DNA oligonucleotide an encapsulating template for the synthesis of AgNCs (Ono et al. 2008). The photoemissive properties of DNA-AgNCs are not only dependent on the number of cytosines, but also affected by the sequences of DNA template, and further influenced by the dimensional structure of DNA template. The photoemissive wavelength of DNA-AgNCs can be tuned by changing the base sequence and length of DNA template. The reported fluorescence of DNA-AgNCs covered the range from visible to near infrared wavelengths (Cerretani et al. 2019). In the earliest work reported by Dickson's lab, DNA-AgNCs with blue, green, yellow and red emission colors were obtained through a random screening process for selecting the favorable synthesizing sequences (Richards et al. 2008). It has been demonstrated that a defined structure like hairpin could help encapsulating silver atoms and endow highly emissive AgNCs (Shah et al. 2016). Qu's group found that highly fluorescent DNA-AgNCs (QY/quantum yield = 33.2%) could be created inside a DNA triplex scaffold, which can provide better protection for AgNCs against quenching in solution (Feng et al. 2012). In our latest work, a nano "DNA bulb" with a spatial structure was employed for the synthesis of DNA-AgNCs, and results showed that the "DNA bulb" could direct clusters' formation, afford fluorescence enhancement, and provide a protective environment (Guo et al. 2018).

Electrochemiluminescence (ECL) is a kind of luminescence with remarkable advantages in applications of analytical chemistry, since its simple instrumentation (does not need expensive excitation optics) and low detection limit (because of low background emission) (Hu and Xu 2010; Liu et al. 2015). The ECL of AgNCs can be excited through an ox–red excitation pathway, in which the AgNCs are first oxidized by cathodically produced oxidizing radicals and then reduced by energetic electrons to the excited form of

their original oxidation state (Díez et al. 2009). The observed ECL emission of DNA-AgNCs can quite be affected by the operating conditions, including coreactant, pH value and excitation pulse amplitude. Qu's group reported that the DNA-AgNCs showed strong ECL emission under lower potential using sodium persulfate ($Na_2S_2O_8$) as the coreactant (Feng et al. 2017). Later the possible ECL mechanism of the reaction between DNA-AgNCs and $S_2O_8^{2-}$ was proposed by Jie et al. (Jie et al. 2017). In this work, Jie et al. observed differential pulse voltammetry (DPV) signal responses with different concentrations of DNA-AgNCs, ascribing to oxidation of DNA-AgNCs on electrode surface (Cao et al. 2019). They developed electrochemical (EL)-based approach and ECL-based approach for the detection of thrombin, respectively. It was found that EL-based approach exhibited lower detection limit (45 times lower) while ECL-based approach showed lower relative standard deviation (better reproducibility). Chen et al. studied the oxidase mimic character of DNA-AgNCs, and discovered the peroxidase-like property of DNA-AgNCs. Instead of the employment of peroxidase-functionalized probes, Chen et al. fabricated a label-free and sensitive electrochemical aptasensor for the amplified determination of lysozyme (Chen et al. 2015a).

Noticeably, the syntheses of AgNCs using DNAs as templates endow the DNA-AgNCs with inherent recognition function of DNA or aptamer. For instance, Yang et al. found that the fluorescence of synthesized DNA-AgNCs diminished when hybridization occurred between template DNA and complementary miRNA, which was proposed for the strategy of a fast and simple detection method for miRNA (Yang and Vosch 2011). Wang's group utilized the aptamer of nucleolin for synthesis of AgNCs, which was employed for imaging of *HeLa* cancer cells (Ai et al. 2012). For DNA probes based on DNA-AgNCs, the recognition unit and signal unit are naturally integrated, no chemical modification or connection was needed, while the employment of conventional fluorescent nanomaterials always suffered a cumbersome process for labeling. The employment of DNA-AgNCs not only reduces the cost of probe preparation and also increases the flexibility of method design. It would be readily couple with some DNA amplification technologies, such as rolling circle amplification (RCA), strand displacement amplification and hybridization chain reaction. For instance, He's lab developed an ultrasensitive DNA detection method with a detection limit of 0.84 pM, which was contributed to the RCA-assisted assembly of DNA-AgNCs (Ye et al. 2014).

As shown in Figure 1(a), the speedy growth curve illustrates the popularity of label-free probes in biosensor development. The term "label-free" was firstly proposed by Josson et al. (Jonsson et al. 1991), who utilized surface plasmon resonance (SPR) method for the study of bio-specific interaction. For exact

definition, direct detections based on spectral methods like Raman, infrared, atomic absorption spectroscopy or gravimetric methods like SPR, piezoelectric microbalance, microcantilever etc. should be regarded as label-free detections (Bier and Scheller 1996; Su et al. 2000; Wu et al. 2001; Fang et al. 2015). The detection signals of these detection methods do not rely on additional signal molecules, but only on the physical properties of the analyte itself. Indirect detections that utilizing fluorescent, electrochemical or radioisotope molecules, that are fixed to the probes by chemical covalent conjugation, for the corresponding output signal are usually regarded as labelled detections (Tyagi and Kramer 1996; Lequin 2005). Compared with chemically labelled probes, the probes that do not require the covalent labeling of additional signal molecules were also reported as label-free probes or biosensors in references (Wang et al. 2009; Kong et al. 2013; Lin et al. 2015; Yi et al. 2020). It refers to the *verb* meaning compared with the previous exact definition, which refers to the *noun* meaning. The SYBR green-based loop-mediated isothermal amplification (Notomi et al. 2000), aggregation-induced emission dye-based polymer probes (Qiu et al. 2019), hemin-based G-quadruplex probes (Zhao et al. 2019) etc. all could be regarded as "label-free" (Guo et al. 2016). By in-situ synthesis on DNA probes, the signal output of AgNCs can be readily realized without the steps of chemical connection, which is reported as label-free signal outputs (Xu et al. 2016; Li et al. 2018; Wu et al. 2018; Liu et al. 2019; Yao et al. 2019). As shown in Figure 1(b), a typical molecular beacon (MB) labelled with fluorophores and a label-free MB using DNA-AgNCs are illustrated. Unlike labelled MB with chemically conjugated signal molecules, the label-free output of DNA-AgNCs-MB can be accomplished just by integrating template sequences at both terminals for in-situ synthesizing AgNCs.

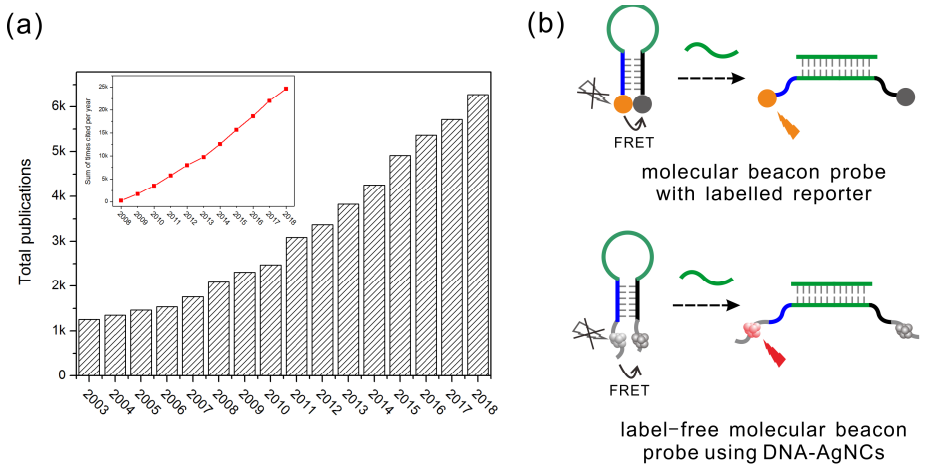

Figure 1. (a) The total number of published articles per year by searching the keywords "label free" in the database of *Web of Science*. Inset*:* the annual citing number per year obtained by searching the keywords

"label free & biosensor" in the *Web of Science* database. (b) Illustration of the labelled MB and label-free MB using DNA-AgNCs as signal output (DNA-AgNCs-MB).

As a kind of label-free signal reporter, DNA-AgNCs have gained great attention in the development of biosensors (Chen et al. 2018a). Heretofore DNA-AgNCs probes have been applied for detecting DNA, miRNA, metal ion, enzyme, pesticide, explosive, cancer cell etc. (Xu and Wei 2017; Li et al. 2018; Zhang et al. 2018a; Shen et al. 2019). In this presented review, most of the related works in recent years were collected to help readers follow the research tendencies. Besides, label-free probes based on DNA-AgNCs signal output were classified by different design strategies for a clear picture, hoping to provide some inspirations to researchers.

2 Label-free probe based on DNA-AgNCs signal output (LFP-DAgNCs)

2.1 LFP-DAgNCs based on direct interaction

The simplest strategy for LFP-DAgNCs application is that the DNA-AgNCs served as both recognition unit and signal output unit based on the direct reaction between the DNA-AgNCs and the targets of interest. As depicted in Figure 2(a), the direct interaction of the targets towards the DNA-AgNCs always resulted in two phenomena: either fluorescence quenching or restored/enhanced fluorescence. For instance, Han et al. found that a more compact structure of the DNA template formed upon the addition of melamine, thus enhancing the fluorescence of DNA-AgNCs (Han et al. 2012). Melamine can bind the thymine of template DNA through hydrogen bonds with a 1:3 stoichiometry. A sensitive detection method for melamine was developed based on this phenomenon. Later in Jeong's work, a LFP-DAgNCs for turn-on detection of melamine was designed based on Hg(II)-induced fluorescence quenching of AgNCs and melamine-induced fluorescence enhancement of DNA-AgNCs (Jeong et al. 2019). The melamine acted as a chelator of preventing Hg(II)-induced quenching, and as an enhancer of boosting the fluorescence of DNA-AgNCs. As shown in Figure 2(b), Wang et al. developed a novel and simple fluorescent "turn-on" sensor for the trace detection of quinolones (Wang et al. 2018a). The principle of the method was based on the fluorescence quenching of the as-prepared DNA-AgNCs by Cu^{2+} ions and the restoration of fluorescence intensity of the DNA-AgNCs-Cu^{2+} system by quinolones. Benefiting from its superior sensitivity, the sensor was available for detection of trace quinolones in tablets and urine with satisfactory recoveries.

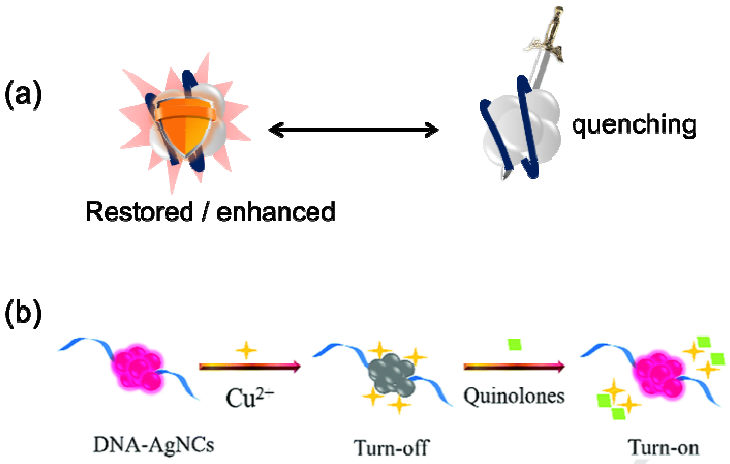

Figure 2. (a) Schematic depiction of the LFP-DAgNCs based on direct interaction. (b) Illustration for the detection of quinolones based on DNA-AgNCs–Cu^{2+} system. (Copyright © The Royal Society of Chemistry 2018)

Using the same strategy, Jia et al. developed an optical platform for highly sensitive detection of alendronate sodium (ALDS) based on Cu^{2+}–mediated fluorescence "on–off–on" evolution of DNA–AgNCs (Jia et al. 2018). The specific binding of Cu^{2+} to DNA-AgNCs induced the quenching of their red fluorescence. In the presence of ALDS, their fluorescence can be restored to a large extent due to the stronger coordination of ALDS with Cu^{2+}. The method was successfully applied to the detection of ALDS in biological samples and pharmaceuticals with a detection limit of 100 pM. As shown in Figure 3, Qin et al. established a simple method for the detection of cytochrome c (Cyt-c) based on fluorescence quenching of DNA-AgNCs as induced by electron transfer between Cyt-c and DNA-AgNCs (Qin et al. 2019). The synthesized DNA-AgNCs were coated with tween 80, resulting in an enhanced fluorescence signal. The detection limit of this method was as low as 0.8 nM. In addition, the prepared DNA-AgNCs probes were used to detect the release of Cyt-c during cell apoptosis, which could provide dynamic information for cell research. In one of our recent work, an excellent short single-strand DNA (ssDNA) that can endow AgNCs with high QY (28%) was discovered through an intended selection process (Guo et al. 2019). And the DNA-AgNCs were employed as visual probes for the fast and sensitive detection of captopril in antihypertensive health food, based on the specific quenching of DNA-AgNCs induced by robust silver-thiol interaction.

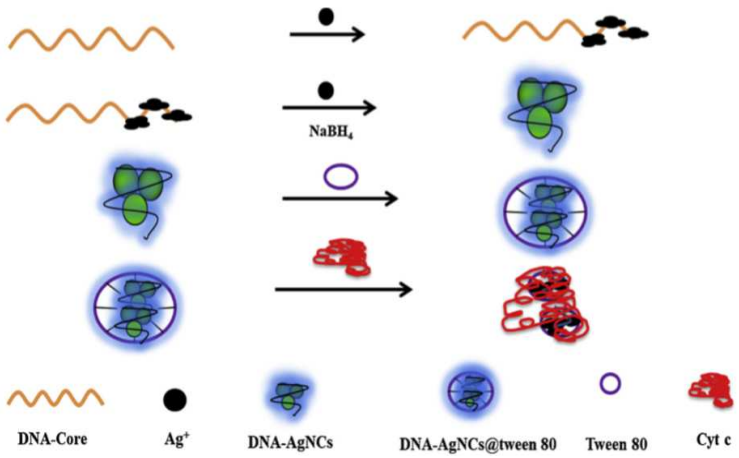

Figure 3. Fabrication of the DNA-AgNCs coated with tween 80 and their application for Cyt c assay. (Copyright © 2019 Elsevier B.V.)

For section summary, the outstanding advantage of this kind of detection strategy is its simplicity, but with limited applicable targets. The change of the fluorescence signal was resulted from the interactions between the silver atoms or DNA template with targets, that are usually metal ions (ex. Hg^{2+}/Cu^{2+}) or small molecules (ex. melamine/cysteine). In our opinion, it will be interesting to explore DNA-AgNCs of using aptamers as templates, especially those aptamers which are selective to certain target cells (Wang et al. 2017b; Wang et al. 2019b). Previous works have demonstrated that the fluorescence of DNA-AgNCs depends on the structure of the synthetic templates (Tao et al. 2018; Ardekani et al. 2019; Shen et al. 2019). Then the structural transformation caused by target-aptamer binding may lead to the change of fluorescence signal, which could be the basic principle for sensor development. This kind of aptamer-AgNCs will definitely promote the development of selective, simple and label-free methods for facile detections.

2.2 LFP-DAgNCs based on indirect interaction

2.2.1 LFP-DAgNCs based on guanines-proximity induced enhancement

Another strategy for the development of LFP-DAgNCs is based on the distance change between DNA-AgNCs and the guanine(G)-rich sequences. Yeh et al. firstly found the intriguing phenomenon that the fluorescence of DNA-AgNCs could be greatly enhanced when they are placed in proximity to G-rich DNA sequences (Yeh et al. 2010; Yeh et al. 2012). Based on this phenomenon, they developed a LFP-DAgNCs for simple and cost-effective identification of a single N^6-methyladenine in a nucleic acid target (Chen et al. 2015b). The basic principle of this method is illustrated in Figure 4(a), when the DNA-AgNCs get close to the G-rich sequence, the fluorescence of DNA-AgNCs would be boosted; while

the long-distance separation would resulted in reduced fluorescence. Zhou's group developed a LFP-DAgNCs for the detection of transcription factor (TF) based on binding-induced conformation allostery and G-proximity induced enhancement (Li et al. 2019a). As shown in Figure 4(b), the probe was subtly designed with a synthesizing sequence at its 5' end and a G-rich sequence at its 3' end. The complementary sequence in blue color was designed for recognizing target TF. In the presence of target, the double-hairpin DNA structure transformed to single-hairpin DNA structure via population shift mechanism, with the assistant binding between TF and recognition sequence. The formation of the single-hairpin DNA structure brought the DNA-AgNCs at 5' end and guanine-rich sequence at 3' end into close proximity, resulting in enhanced fluorescence for analytical quantification. This method can be applied in detecting endogenous TFs in cell samples with simple procedures yet excellent performances.

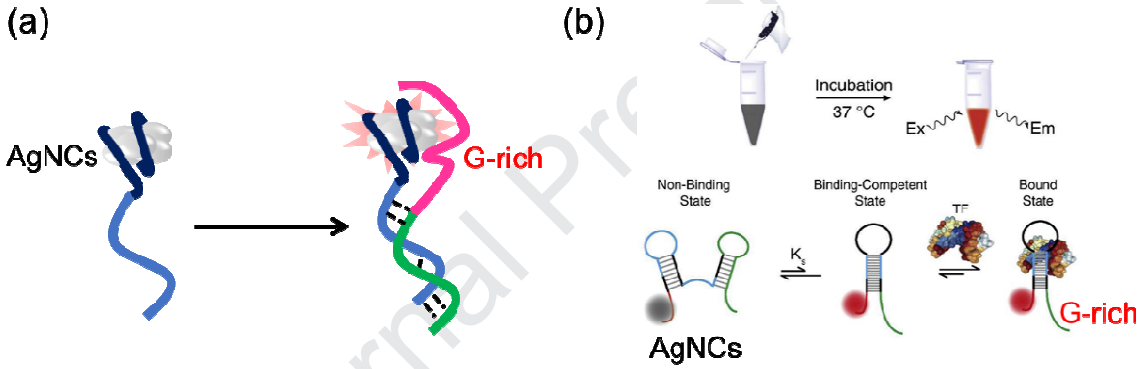

Figure 4. (a) Schematic depiction of the LFP-DAgNCs based on G-proximity induced enhancement. (b) The detection of TF using LFP-DAgNCs based on binding-induced conformation allostery and G-proximity induced enhancement. (Copyright © 2019 Elsevier B.V.)

Yan et al. designed a molecular beacon-based fluorescent probe to determine the cancer drug bleomycin (BLM) based on G-proximity induced enhancement of DNA-AgNCs (Yan et al. 2018). As shown in Figure 5(a), the label-free probe was designed with DNA-AgNCs and G-rich sequences on both terminals. In the absence of the BLM-Fe(II) complex, the probe held a hairpin shape and showed strong fluorescence due to the G-proximity. In the presence of the BLM-Fe(II) complex, which will selectively cleave the probe at the 5'-GC-3′ scission site of the loop. This resulted in the separation of the DNA-AgNCs from the G-rich sequence, causing a decreased fluorescence. The detection limit of this method was as low as 33 pM, which was 1-3 orders of magnitude higher than the sensitivity reported in most literatures. This probe was used for the measurement of BLM in human serum, and good results were obtained. Using the same design strategy, Ma et al. proposed a method for the detection of alkaline phosphatase (ALP) based on G-rich

induced light-up phenomenon and exonuclease (λ-Exo) cleavage reaction (Ma et al. 2018). When λ-Exo was added, the G-rich DNA was cleaved and the DNA-AgNCs was separated from G-rich sequences, thus resulting in fluorescence decrease. While the treatment by ALP would cause the hydrolysis of the 5'-phosphoryl end of G-rich DNA, preventing the λ-Exo cleavage reaction.

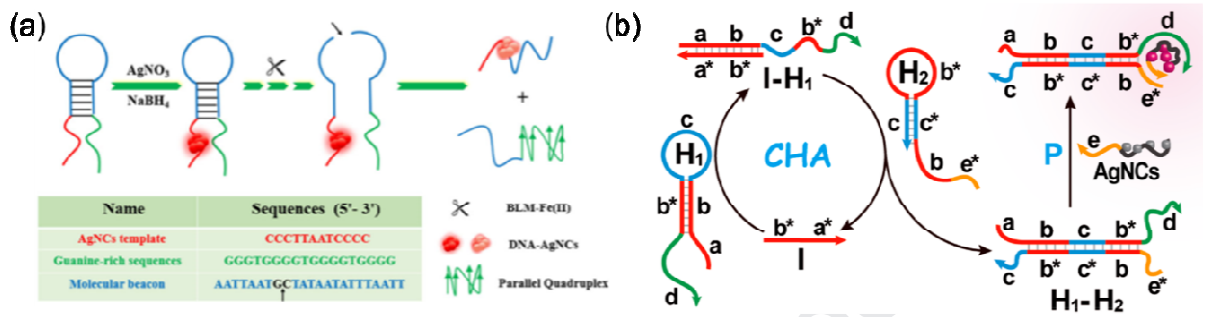

Figure 5. (a) Illustration of a LFP-DAgNCs for the detection of BLM based on strand scission and G-proximity induced enhancement. (Copyright © Springer-Verlag GmbH Austria, part of Springer Nature 2018). (b) Scheme of the CHA-mediated amplified DNA assay based on G-proximity induced lighting up of dark DNA-AgNCs. (Copyright © 2018, American Chemical Society).

Catalytic hairpin assembly (CHA) is a method of catalyzing the cross-opening of two hairpin substrates by an initiator. Pan et al. constructed a label-free and enzyme-free isothermal CHA-based method for DNA detection with high sensitivity and selectivity (Pan et al. 2018). As shown in Figure 5(b), the strategy designed a hairpin grafted with a G-rich sequence and a hairpin captured by another AgNCs into an assembly. In the presence of the target, the CHA-catalyzed assembly of two functional hairpins was carried out one after the other, accompanied by efficient regulation of the elongated double-stranded DNA (dsDNA) products of AgNCs and G-rich sequences, yielding efficient AgNCs-lighting and amplification of the fluorescent signal. This strategy provided a simple visualization method for DNA amplification detection with a detection limit of 20 pM.

For section summary, G-proximity enhancement provides a simple mode for label-free and turn-on detection, which is similar to the dual-labeling probes. Combined with the aptamer sequences, simple LFP-DAgNCs can be easily developed for molecule detections (Zhou et al. 2011; Li et al. 2012; Zhang et al. 2012b; Zhang et al. 2019b). Besides, with the assistance of some signal amplification strategies, the signal can be further amplified to implement more sensitive measurements. While the fundamental principles of this enhancing phenomenon are still unclear, the applications of LFP-DAgNCs will definitely be explored and the underlying mechanisms will be investigated and clarified.

2.2.2 LFP-DAgNCs based on FRET-induced quenching

Fluorescence resonance energy transfer (FRET) is a principle describing energy transfer between two photoemissive fluorophores or between a fluorophore and an energy donor (Zhang et al. 2012a). As a kind of fluorophore, DNA-AgNCs can also undergo the FRET phenomenon and thus be designed into versatile detection strategies for developing LFP-DAgNCs. As shown in Figure 6(a), Jiang et al. developed a fluorescence method for simultaneous detection of alpha-fetoprotein (AFP) and carcinoembryonic antigen (CEA) based on the FRET principle (Jiang et al. 2019b). In the absence of targets, the aptamers of AFP and CEA were in a relaxing state and could be adsorbed on the surface of the polydopamine with strong affinity through π–π stacking, which resulted in the fluorescence quenching of aptamer-DNA-AgNCs through the FRET principle. In the presence of target tumor markers (AFP or CEA), the aptamer-DNA-AgNCs would be released from the polydopamine by forming a more stable aptamer/target complex. Therefore, fluorescence could be recovered. The unique property of the sequence-dependent wavelength contributed to the feasibility of multiplex detection. Miao et al. developed an amplification detection strategy for microRNA (miRNA-155) detection based on the FRET and the recycling signal amplification assisted by duplex-specific nuclease (DSN) (Miao et al. 2018). As shown in Figure 6(b), positively charged AuNPs ($AuNPs^{+}$) were prepared using sodium borohydride and cetyltrimethylammonium bromide, which acted as a quencher when electrostatically adsorbing onto the negatively charged ssDNA or DNA−RNA heteroduplexes. In the presence of DSN, the fluorescent DNA-AgNCs part will be liberated with a restored fluorescence intensity due to the enzymatic hydrolysis of the DNA strand in the heteroduplexes. Detection limit of femtomolar level was achieved taking advantages of the high quenching efficiency of $AuNPs^{+}$ and the DSN-assisted target cycling.

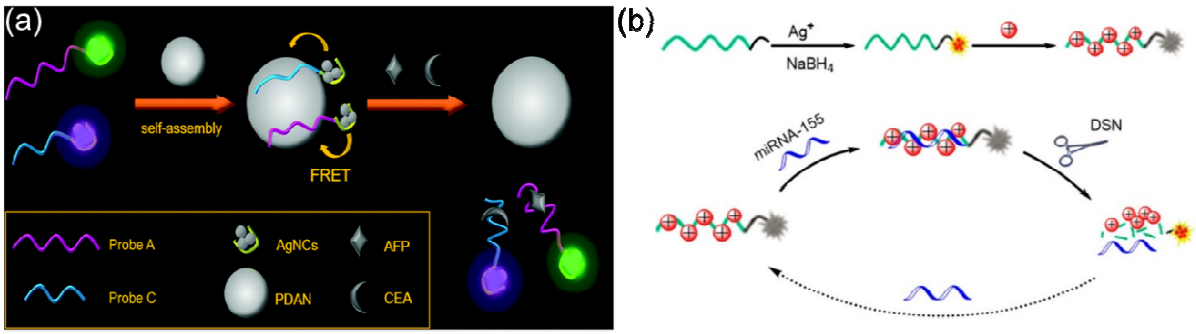

Figure 6. (a) Depiction of the FRET-based LFP-DAgNCs for the detection of multiplex tumor markers by using polydopamine as quencher. (Copyright © The Royal Society of Chemistry 2019). (b) Illustration of the amplification strategy for miRNA-155 detection based on FRET and DSN-assisted recycling signal

amplification. (Copyright © 2018, American Chemical Society).

Borghei et al. established a LFP-DAgNCs for detecting human BRCA1 gene deletion fragments based on FRET between DNA and CdTe quantum dots (QDs) (Borghei et al. 2018). In the presence of target DNA, hybridization of the dsDNA caused the DNA-AgNCs and CdTe QDs to be in close proximity due to the intercalation of CdTe QDs into dsDNA. In this model, DNA-AgNCs acted as energy donor and QDs acted as energy acceptor. This fluorescent FRET-based LFP-DAgNCs exhibited high sensitivity with a detection limit of 12 pM. Zhu et al. reported a new type of LFP-DAgNCs based on enzyme-polymerized polyadenylic acid (poly-dA) DNA chain and front-end strand displacement reaction, which could effectively label genomic DNA fragments in cells (Zhu et al. 2018). The expressed strand triggered by the target led to the release of the quencher labelled DNA from DNA-AgNCs probe, resulting in significant restored fluorescence of DNA-AgNCs with high signal-to-background ratio (S/B = 58). In addition, the authors demonstrated the feasibility of the method by in-situ quantitative analysis of apoptosis in HepG2 cells without the need for cumbersome washing and separation steps. BRCA1 (breast cancer 1) gene deletion is the most important initiator mutation in breast cancer patients.

For section summary, such FRET-based strategies always employed nanomaterial or labelled molecule as a quencher. The effectiveness of the detection depends on the efficiency of FRET and the QY of the DNA-AgNCs. The utilization of enzyme-assisted amplification techniques will promote a better detection capability.

2.2.3 LFP-DAgNCs based on nanocluster dimer

As shown in Figure 7(a), Liu et al. studied the fluorescence enhancement phenomenon in the process of approach between two DNA-AgNCs (Liu et al. 2017). It was termed nanocluster dimers (NCD) when the two AgNCs were squeezed with each other, and the fluorescence intensity of NCD was sensitive to the distance between two DNA-AgNCs. Obvious fluorescence enhancement was observed in the hybridization-induced formation of NCD structure. And it was found that the fluorescence intensities of the NCD decreased gradually with the increasing number of nucleotides spacers and mismatched bases. As the position of single mismatched base moved gradually from the middle point to the end of the target DNA (P1-P17), the fluorescence intensities of the NCD decreased when the position of single mismatched base moved from P1 to P13 due to the decreasing hybridization reaction rates and increasing *Gibbs* binding free energy, while increased from P14 to P17 due to the sufficient hybridization for the sandwich NCD structure.

Based on this phenomenon, a universal platform to pinpoint various SNP positions was developed. The recorded excited-state emission lifetimes indicated that the lifetime of two AgNCs got shorter after they got close, which suggested possible interactions of plasmonics effect. Miao's lab developed a LFP-DAgNCs for ratiometric detection of miRNA based on the formation of NCD and hybridization chain reaction (Jiang et al. 2019a). They designed a hairpin probe of containing two DNA templates at terminals that are in close proximity. In an original state, the synthesized two terminal DNA-AgNCs produced red emission due to the formation of NCD. Hybridization with the auxiliary DNA would result in separation of the two segmental terminal DNA-AgNCs, accompanied with a color switching from red to yellow. The target-triggered successive assembly of auxiliary DNA and hairpin probe contributed amplified signals based on hybridization chain reaction.

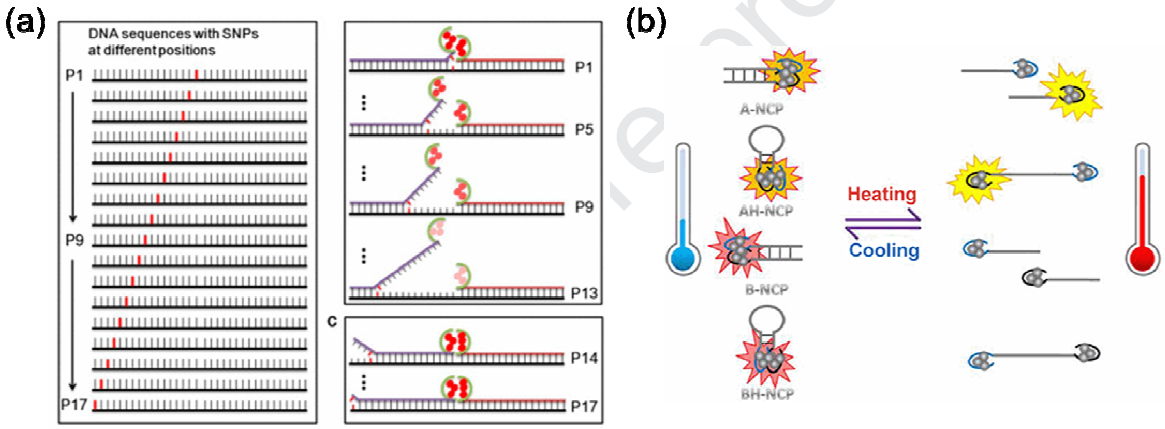

Figure 7. (a) Schematic illustration of different the NCD-based LFP-DAgNCs for pinpoint the position of single nucleotide polymorphism. (Copyright © 2017, American Chemical Society) (b) Schematic design of the two-kinds of temperature-sensitive LFP-DAgNCs. (Copyright © 2018, Tsinghua University Press and Springer-Verlag GmbH Germany, part of Springer Nature)

Dong's lab reported a type of dual-emission LFP-DAgNCs that showed sensitive response towards temperature change from 15 to 45 °C (Zhou et al. 2018). As shown in Figure 7(b), the authors developed two kinds of temperature-sensitive LFP-DAgNCs based on the NCD formation by bringing two DNA-AgNCs together. The temperature-sensitive responses were caused by the temperature-induced hybridization/dehybridization of the two segments of C-rich DNA-templated AgNCs. The integrating and separating of the two segmental DNA-AgNCs at terminal resulted in different fluorescence changes: for A-NCP and AH-NCP a ratiometric response; for B-NCP and BH-NCP, the dual fluorescence emissions of two DNA-AgNCs declined simultaneously as temperature increased. The AgNCs pairs were applied for detecting temperature variations in living breast cancer cells (MCF-7). Han et al. developed a

multifunctional fluorescent probe for simultaneous detection of multiple targets based on G-quadruplex and DNA-AgNCs (Han et al. 2019). In the work, a probe with two recognition regions was designed with a blocked G-quadruplex and dark DNA-AgNCs at each terminus respectively. Upon the addition of target DNA/RNA 1, enhanced fluorescence signals of thioflavin T would generate due to the formation of G-quadruplexes. After binding with target DNA/RNA 2, free cDNA-AgNCs in solution could hybridize with the DNA-AgNCs of probe, resulted in the formation of NCD with enhanced fluorescence signals.

For section summary, the DNA-AgNCs dimers have been emergingly reported in the past two years, but the phenomena are dubious (unvaried/color switching/diminishing) and fundamental mechanism has not been clarified. The study of DNA-AgNCs dimers is definitely an interesting and meaningful research, and it will also be conducive to the development of LFP-DAgNCs.

2.2.4 LFP-DAgNCs based on the formation/destruction of DNA template

This kind of probes was generally designed by two ways: (I) blocking/liberation of synthesizing sequence; (II) hydrolysis/integrity of synthesizing DNA template. The Figure 8 showed a typical LFP-DAgNCs based on the formation of DNA template, as proposed by Zhang's group (Zhang et al. 2015). The sequences for syntheses of green-emitting and orange-emitting AgNCs were engineered into two DNA hairpin probes respectively, which were both blocked due to the formation of stem-loop structure. The presence of corresponding target DNAs resulted in the open of the hairpin probes because of complementary hybridization, thus releasing the sequences for synthesis. The emission wavelengths of the two kinds of AgNCs were 507 nm and 597 nm respectively, and the output signals did not interfere with each other, contributing to the interesting two-color detection. Kim et al. developed a LFP-DAgNCs to detect the Klenow fragment exo$^-$ (KF$^-$) activity and to monitor its inhibition with daidzein based on the blocking of a hairpin DNA template for DNA-AgNCs synthesis (Kim and Gang 2019). The hairpin DNA consisted of a 9-cytosine loop, a 6-pair stem region and a trailing 8-base ssDNA as polymerization template. In the absence of KF$^-$, the DNA-AgNCs cannot form because the hybridization with cDNA disrupted the stem region of hairpin DNA, and the bright DNA-AgNCs cannot be synthesized without a complete hairpin DNA template. In the presence of active DNA polymerase, polymerization would be carried out and cDNA cannot open the stem region of the hairpin DNA, resulting in a completed hairpin DNA template for synthesis of bright DNA-AgNCs. The detection limit of this method was 0.05 U/mL. In addition, the concentration of daidzein can be detected due to the inhibitory effect towards KF$^-$.

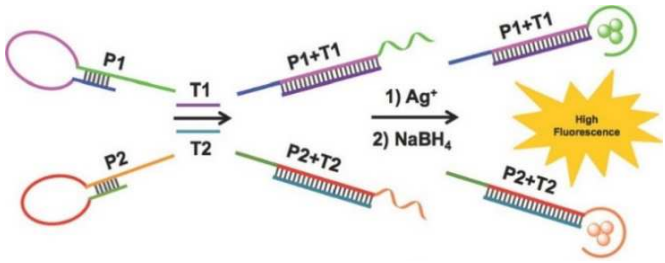

Figure 8. Two-color strategy for multiple DNA detections using LFP-DAgNCs based on the liberation of hairpin templates. (Copyright © 2014 WILEY-VCH Verlag GmbH & Co. KGaA, Weinheim.)

To illustrate a typical LFP-DAgNCs based on the hydrolysis/integrity of synthesizing DNA template, as shown in Figure 9(a), Ye's group developed a sensitive method for detecting nicotinamide adenine dinucleotide (NAD^+) using LFP-DAgNCs (Wang et al. 2017a). A dumbbell-shape DNA template containing two C-rich loops was employed for the synthesis of AgNCs, and two DNA enzymes were employed for reducing the background signal by digesting the template completely. In the presence of NAD^+, it acted as the cofactor of DNA ligase and sealed the dumbbell-shape DNA template in the nick site, which would not be digested by Exo-III and Exo-I. Thus, highly fluorescent AgNCs could be synthesized in this two-loop template. In the absence of NAD^+, the ligation reaction would not occur due to the lack of cofactor, and the unsealed dumbbell-shaped template would be digested by Exo-III and Exo-I. Fluorescence would not be generated without the DNA template. So, the generation of fluorescence depended on the ligation of the dumbbell template, making the principle of the detection strategy. Tang et al. proposed a LFP-DAgNCs for the ultrasensitive detection of mercury (II) (Hg^{2+}) by employing enzyme-assisted amplification strategy (Xu et al. 2016). As shown in Figure 9(b), they designed a half-open hairpin probe with thymine–thymine (T–T) mismatches in the end of the stem part. In the absence of Hg^{2+}, the hairpin DNA acted as a complete template for synthesizing of AgNCs to generate fluorescence signal. After addition of Hg^{2+} into the detection system, Hg^{2+} specifically coordinated with T-T mismatches to form an intact stem dsDNA with blunt termini, resulting in the digestion by Exo-III and destruction of the hairpin structure. Then Hg^{2+} would be liberated and initiated the next cycling of digestion process. This method showed a dynamic range from 0.1 nM to 10 nM towards Hg^{2+} with a detection limit of 24 pM.

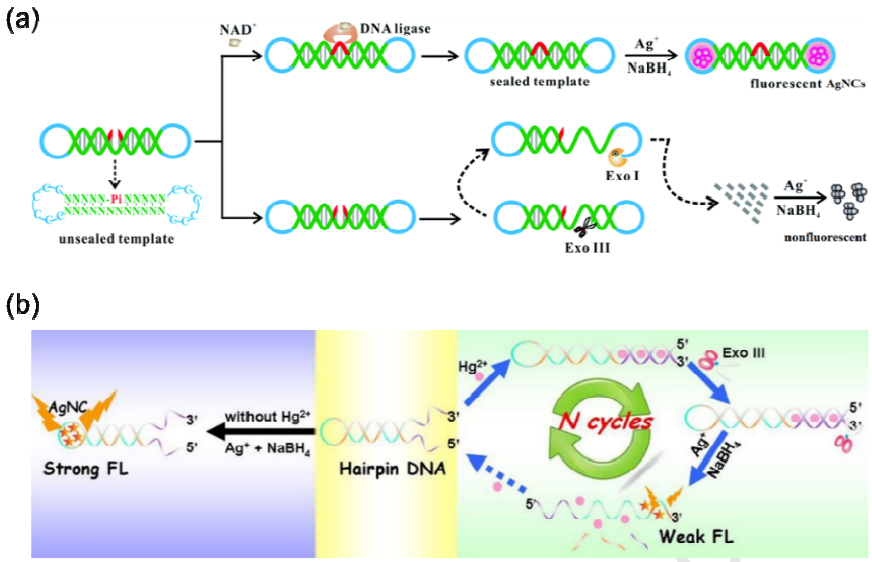

Figure 9. (a) Sensitive detection of NAD^+ based on dumbbell-shape DNA templated DNA-AgNCs and enzyme-assisted amplification. (Copyright © The Royal Society of Chemistry 2017) (b) A LFP-DAgNCs for the ultrasensitive detection of Hg^{2+} by employing enzyme-assisted amplification. (Copyright © 2016 Elsevier B.V.)

For section summary, the LFP-DAgNCs based on blocking/liberation strategy is a kind of label-free molecular beacon with unique advantages in multi-target detection. Polychromatic probes can be easily designed only by employing different synthesizing sequences, while without the labeling process of multiple luminophores. Besides, it was found that LFP-DAgNCs based on hydrolysis/integrity of DNA template demonstrated excellent detection results when combined with exonuclease-assisted amplifications, which provided a good tactic for the development of LFP-DAgNCs.

2.2.5 LFP-DAgNCs based on the assembly on sensor surface

Hybridization chain reaction (HCR) is one of the most popular enzyme-free strategy for signal linear amplification (Dirks and Pierce 2004). As shown in Figure 10(a), HCR is based on chain reaction of recognition and hybridization between alternating complementary sequences. This kind of end-to-end cross-complementary hybridization drives a self-assembly process, leading to the formation of linear-type DNA nanostructures with nicked double helixes (Bi et al. 2017). Peng et al. developed an ultrasensitive detection of methyltransferase activity using an electrochemical LFP-DAgNCs based on electrochemical reduced graphene oxide/AuNPs hybrids and HCR (Peng et al. 2018). As shown in Figure 10(b), in the presence of methyltransferase, the specific recognition sequence on the partial dsDNA will be methylated and then be digested by DpnI, thus the HCR process cannot proceed. While in the absence of methyltransferase, the hanging part of dsDNA on the electrode surface will hybridize with DNA1 and

DNA2 continuously to form the linear-type superstructure, with numerous AgNCs in-situ generated on the cytosine-rich sequences of DNA1 and DNA2. The content of Dam MTase could be sensitively analyzed according to the electrochemical signal output.

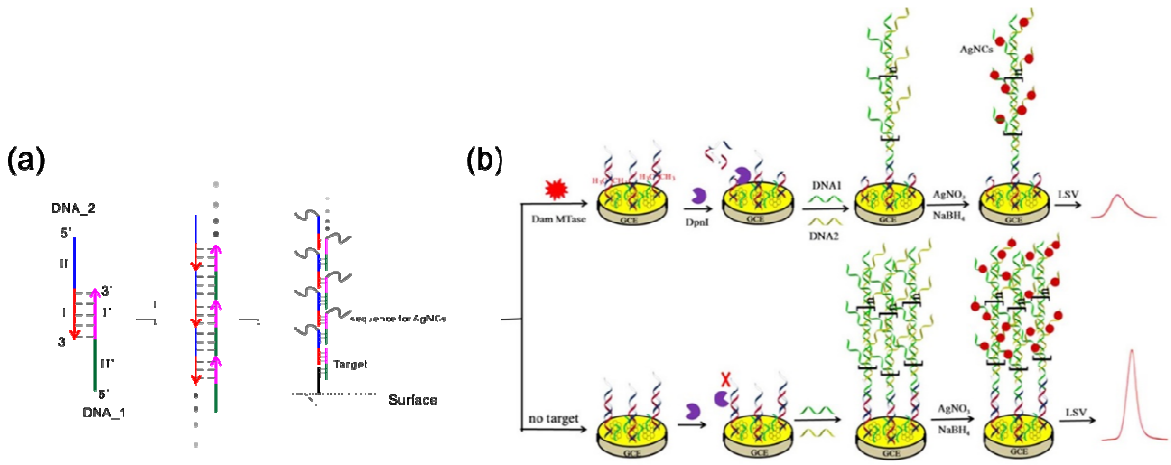

Figure 10. (a) Design principle of the amplification detections based on HCR using DNA-AgNCs as label-free reporters. (b) Schematic depiction of the electrochemical sensor for the amplified detection of methyltransferase activity using LFP-DAgNCs based on HCR-induced surface assembly. (Copyright © 2018 Elsevier B.V.)

As mentioned in that case, HCR is a very simple and direct technology for the surface enrichment of nucleic acid, which is perfectly suitable for surface modification and signal amplification of electrochemical detections. Especially when it is coupled with DNA-AgNCs, ultrasensitive and label-free electrochemical sensors can be developed. As shown in Figure 11(a), Yang et al. proposed a label-free, highly sensitive and selective miRNA-199a electrochemical LFP-DAgNCs based on target-assisted polymerization nicking reaction (TAPNR) and HCR amplifications (Yang et al. 2015). In the TAPNR process, the target miRNA-199a hybridized with the amplification template probe, which contained three regions: target-binding domain, recognition domain of restriction endonuclease and amplification template domain for producing massive intermediate sequences. The hybridization between target miRNA-199a and the probe initiated the TAPNR process to produce massive intermediate ssDNAs with the assistance of Bst-DNA polymerase and Nt.BbvCI restriction endonuclease. The released intermediate ssDNAs were then captured by the HCR probes on the gold electrode surface, and further triggered HCR amplification to form linear-type nanostructures with numerous C-rich loop templates for AgNCs synthesis. DNA-templated synthesis of AgNCs can be in-situ realized by subsequent incubation of the numerous templates with $AgNO_3$ and sodium borohydride. The amount of in-situ synthesized AgNCs was significantly enhanced by

the integrated dual amplification strategies, resulting in a dramatically amplified current response for highly sensitive detection with a detection limit of 0.64 fM. Chen et al. developed a highly sensitive LFP-DAgNCs for DNA detection based on autocatalytic strand displacement amplification (ASDA) and HCR (Chen et al. 2018b). As shown in Figure 11(b), the target recognition opened the immobilized hairpin probe (IP) and initiated the binding of the auxiliary DNA strand (AS) with the opened IP for the successive polymerization and nicking reaction in the presence of DNA polymerase and nicking endonuclease. This induced the target recycling and generation of a large amount ssDNA with the same sequence as target DNA to execute more reactions. Simultaneously, the introduced AS strand can trigger the HCR process with the assistance of two hairpins to form linear DNA concatamers with cytosine-rich templates, which facilitated the in-situ syntheses of DNA-AgNCs as electrochemical tags. This ultrasensitive LFP-DAgNCs had a detection limit as low as 0.16 fM, showing potential for low-abundance nucleic acid detection.

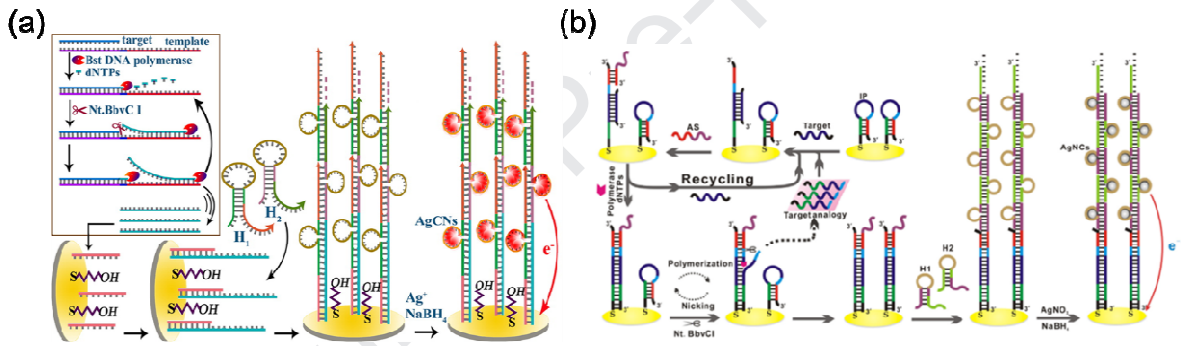

Figure 11. (a) Schematic illustration of ultrasensitive and label-free electrochemical detection of miRNA-199a based on in-situ generated DNA-AgNCs by coupling TAPNR with HCR amplifications. (Copyright © 2015 American Chemical Society) (b) Schematic illustration of the cascade ASDA and HCR strategy for nucleic acid biosensing. (Copyright © 2018 Elsevier B.V.)

Wu et al. proposed a imaging platform for cell surface glycans based on LFP-DAgNCs and HCR (Wu et al. 2018). For the construction of this platform, artificial sugars with azide groups were labelled to the cell surface using the metabolic glycan labeling technique (Sun et al. 2018), and the dibenzocyclooctyne (DBCO)-functionalized DNA probes were immobilized on the surface by reacting with azide groups through copper-free click chemistry. As shown in Figure 12, after the fix of DNA probes on the cell surface, the HCR process was activated with assistance of two hairpin DNAs and linear DNA concatamers with numerous DNA templates were generated for synthesis of fluorescent DNA-AgNCs. This signal amplification strategy was used in quantitative analysis, and the detection limit was as low as 20 cells in 200 μL of binding bu□er. In addition, the DNA-AgNCs had significant photothermal performance due to

the HCR-induced formation of super nanostructure, which could effectively kill cancer cells and inhibit the growth of tumors under image guidance. In this method, the HCR process avoided the introduction of excessive azide sugar on the premise of ensuring apparent fluorescence. These results indicated that the developed nano-platform has great potential for specific cell surface glycan imaging and fluorescence-guided photothermal therapy. Using a similar strategy, Zhang et al. also developed a fluorescence LFP-DAgNCs based on HCR technique (Zhang et al. 2017). The developed sensor was employed to detect human immunodeficiency virus-related DNA sequences in vitro with a detection limit of 1.18 nM. Graphene oxide was utilized to decrease the background signal.

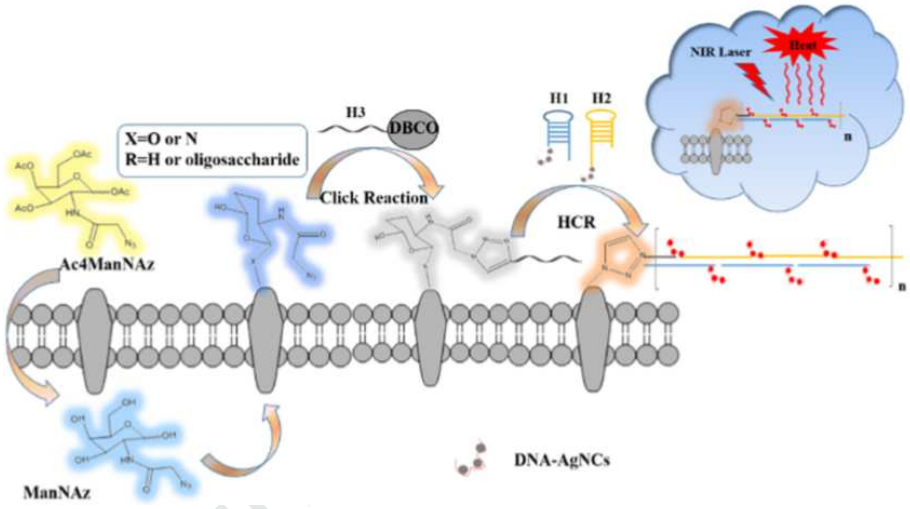

Figure 12. Schematic illustration of the HCR-based theranostic nanoplatform for label-free fluorescence imaging of cell surface glycans and fluorescence guided photothermal therapy. (Copyright © 2018 American Chemical Society).

For section summary, the HCR is an ideal technique to enrich DNA-AgNCs on the sensor surface to generate label-free signals, especially on the surface of electrodes. In addition to HCR, RCA is also an applicative technique for enriching DNA templates on the surface of sensors. For instance, Chen et al. developed an ultrasensitive electrochemiluminescence LFP-DAgNCs for miRNA detection based on three-junction assisted RCA as a surface enriching technique for signal amplification (Chen et al. 2016a). These surface enrichment technologies not only achieve the output of the detection signal, but also amplify the signal readout. In addition, in-situ synthesized DNA-AgNCs bear inherent label-free merit, eliminating the tedious labelling process of signal reporters like electrochemically active molecules. Overall, this kind of LFP-DAgNCs shows great potential for development of highly sensitive and label-free sensors.

2.3 LFP-DAgNCs for imaging of cancer cell

Figure 13(a) illustrated a typical design of LFP-DAgNCs for direct cancer cell imaging application. The DNA-AgNCs carrying aptamer sequence could recognize cancer cells via the specific binding towards overexpressed markers on the cell surface. By conjugating the aptamer sequence of anterior gradient protein 2 homolog (AGR) and a cytosine-rich sequence, Lan et al. developed a label-free probe for imaging breast cancer cells (Lan et al. 2019). The sequence of this imaging probe consisted of two functional units, aptamer sequence for targeting the AGR on breast cancer cells as recognition unit, and twelve-cytosine sequence for preparing AgNCs as signal output unit. The as prepared AgNCs emitted orange fluorescence with a maximum emission peak at 565 nm and a QY as high as 87.43%. MTT assay was carried out to evaluate the biocompatibility, which indicated that the synthesized DNA-AgNCs had a low toxicity. As shown in Figure 13(b), confocal images exhibited that the as-prepared DNA-AgNCs gathered nearby nuclei and distributed along a line from the nuclei to the cell membrane. The position of gathering nanoclusters can be seen as AGR's secretion process, indicating that the probe successfully targeted to the AGRs in MCF-7 cells.

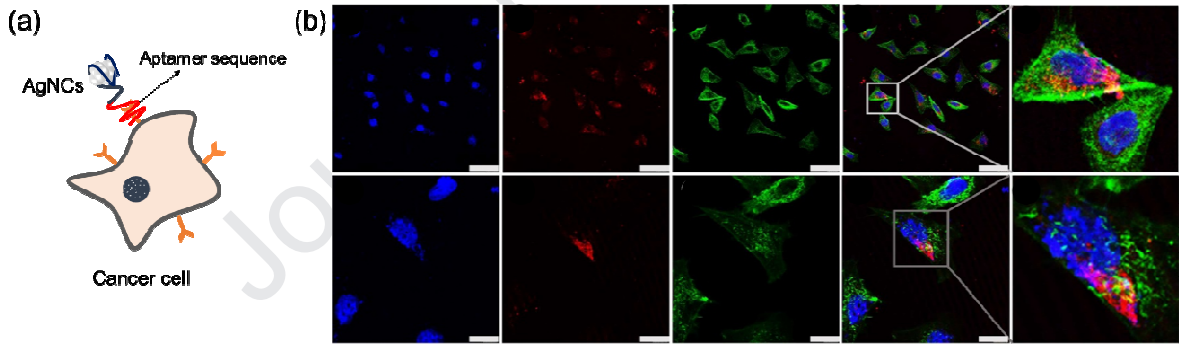

Figure 13. (a) Schematic depiction of the electrochemical sensor for the detection of methyltransferase activity using LFP-DAgNCs. (b) Confocal microscopy images of MCF-7 cells. The cells were stained with (from left to right): Hoehcst-33258, AgNCs-based DNA probe, Alex Fluor 488, merged images and 6/4 times amplification of merged images respectively. (Copyright © 2019 Elsevier B.V.)

Zhu et al. constructed a novel nanocomposite with cancer-specific imaging and targeted therapeutic functions by assembling DNA-AgNCs around DNA-modified gold nanoparticles (AuNPs) (Zhu et al. 2017). The as-prepared nanocomposite carries a high-density of AS1411 aptamer, which was the first anti-cancer aptamer of targeting overexpressing nucleolin on cancer cell surface. The as-prepared AuNP@(AS1411–AgNCs)n nanocomposite showed strong near-infrared fluorescence emission with a high density of fixed aptamers on surface. The synergistic effect of AS1411-guided binding and internalization

led to specific cell imaging and selective killing. On the contrary, normal NIH-3T3 cells without over-expressed nucleolin on the surface showed weak fluorescence signal. The results suggested that the as-prepared nanocomposites could be used for imaging of highly specific cancer cells. By using carbohydrate instead of aptamer, Zhang et al. utilized carbohydrate-modified DNA as a template for the synthesis of DNA-AgNCs (Zhang et al. 2018b), which were employed for cancer cell imaging based on the recognition of mannose with mannose receptor on cancer cells MDA-MB-231. The MDA-MB-231 and 293T cells were selected as parallel-controlled target cells. The 293T cells were incubated with the DNA-AgNCs but no fluorescent signal was observed, while the MDA-MB-231 cells showed strong emissive signal in fluorescence images, showing excellent selectivity.

For section summary, the DNA-AgNCs with aptamer sequences are economical and effective probes for cancer cells imaging. A wide variety of specific aptamers of targeting cancer cell have been screening out through a SELEX (systematic evolution of ligands by exponential enrichment) process (Zhu et al. 2012; Pereira et al. 2018), such as leukemia cells (Shangguan et al. 2006), papillary thyroid carcinoma (Zhong et al. 2019), cervical cancer (Wang et al. 2019b) and renal cell carcinoma (Wang et al. 2017b), etc. The aptamer-DNA-AgNCs with targeting characteristics can be specifically enriched to the surface of cancer cells for imaging, which are different from conventional organic dyes or fluorescent nanomaterials without specificity. By simple integration of targeting sequence and synthesizing sequence, the most highlighted advantage of aptamer-DNA-AgNCs is that cumbersome labelling process is avoided.

3 Discussion and perspective

In the past five years, tremendous literatures on the applications of DNA-AgNCs have been reported. In this presented review, just some typical examples were listed for explaining different design strategies. Some recently reported detection methods using LFP-DAgNCs were listed in the appendix of this review. It is expected that with the recognition of the advantages of DNA-AgNCs by more researchers, emerging excellent work will be reported in the near future.

To conclude, this review focuses on the label-free probes based on DNA-AgNCs signal output. The LFP-DAgNCs do not require expensive and cumbersome modification, which contributed the low-cost and simple outputs. Besides, the signal output mode is versatile, which is beneficial to design a variety of detection strategies. Previous reported works have evinced the versatile performances of LFP-DAgNCs in fluorescence and electrochemical methods. Besides, unlike conventional label-free fluorescent dyes, the

LFP-DAgNCs can enable selective signal output when responding to multiple targets. For instance, for the detection of two different DNA targets in one solution, the employment of SYBR-green only generate green fluorescence; while in LFP-DAgNCs-based detection methods different colors can be obtained by designing different synthesizing sequences for AgNCs. It is firmly believed that the LFP-DAgNCs will demonstrate this advantage for multi-target and multi-color detection in the future. In addition, in combination with enzyme-assisted or enzyme-free amplification strategies, the sensitivity of LFP-DAgNCs can be improved.

The stability of DNA-AgNCs is now a grave concern of DNA-AgNCs that have been suffering from photobleaching and short shelf life. One of the reasons for the fragility is that most reported DNA-AgNCs used ssDNAs templates (Guo et al. 2019), which cannot fully package the silver atoms. Our research team recently reported a research work in which we used a three-dimensional spatial structure of DNA template for the synthesis of AgNCs (Guo et al. 2018). The results of a series of studies showed that this structure could bring enhanced fluorescence of DNA-AgNCs, and promote the storage stability of DNA-AgNCs. This study enlightened the idea of synthesizing AgNCs in different DNA nanostructures with spatial structures. Zhou et al. presumed that temperature-induced oxidation could cause non-reversible decrease in the fluorescence of DNA-AgNCs, and they found that the fluorescence recovered after adding a small quantity of $NaBH_4$ to the solution of DNA-AgNCs (Zhou et al. 2018). It is of great significance to study the synthesis of more stable DNA-AgNCs for promoting wider researches and practical applications. Spatial DNA templates and employment of additional antioxidant ligands may provide solutions to help solve this problem.

4 Appendix: recently reported biosensors using LFP-DAgNCs.

Strategy	Target	Highlight	Detection limit	Ref.
Direct interaction	ascorbic acid & ascorbic acid oxidase	dual-model	0.6 μM & 0.0048 U/mL	(Liu and Pang 2018)
	cysteine	simple	0.05 nM	(Wang et al. 2018b)
	pyrophosphate ions	simple	0.28 μM	(Xu et al. 2019)
	melamine	simple	49 nM	(Jeong et al. 2019)
	captopril	simple	0.05 μg/mL	(Guo et al. 2019)
	tiopronin	simple	270 pM	(Zhang et al. 2019d)
	glucose	simple	not provided	(Schroeder et al. 2019)
	Hg^{2+}	DNA-Cu/AgNCs	2.4 nM	(Mao and Wei 2019)
	UO_2^{2+} & Hg^{2+}	hairpin DNA template	1.8 pM & 0.1 nM	(Lin et al. 2019)
Indirect interaction (guanines-proximity induced enhancement)	DNA	ratiometric detection based on DNA radar structure	0.52 nM	(Wang et al. 2019d)
	T4 polynucleotide kinase	kinetic determination	0.01 U/mL	(Li et al. 2019b)
	terminal deoxynucleotidyl transferase	convenient	0.8 mU/mL	(Chi et al. 2019)
	transcription factor	simple	2 nM	(Li et al. 2019a)
	human epidermal growth factor receptor-2	ultrasensitive	0.0904 fM	(Zhang et al. 2019b)
	Zn^{2+} in cell	three-way DNA junction	0.023 nM	(Yao et al. 2019)
Indirect interaction (FRET-induced quenching)	miRNA-21	quencher (BHQ1)	0.61 nM	(Lu et al. 2018)
	miRNA-155	positively charged AuNPs	33.4 fM	(Miao et al. 2018)
	Hg^{2+}	positively charged AuNPs	2.3 pM	(Ma et al. 2019)
	kanamycin	AuNPs	1.0 nM	(Ye et al. 2018)
	E. coli O157:H7	AuNPs	0.0019 CFU/mL	(Wang et al. 2019a)
	uracil-DNA glycosylase	AuNPs	0.1 mU/mL	(Zhang et al. 2019a)
	IFN-γ & adenosine & thrombin	polypyrrole nanoparticle	0.58 & 0.39 & 2.2 nM	(Wang et al. 2019c)
	AFP & CEA	polydopamine nanoparticle	2.4 & 5.6 nM	(Jiang et al. 2019b)
	telomerase in cancer cell	parallel G-quadruplex	15 cells/μL	(Lee et al. 2019)
Indirect interaction (nanocluster dimer)	single nucleotide polymorphisms	color diminishing	point mutation	(Liu et al. 2017)
	temperature	color switching / diminishing	not provided	(Zhou et al. 2018)
	DNA/RNA	color diminishing	0.45 nM	(Han et al. 2019)

	miRNA	color switching	2.8 pM	(Jiang et al. 2019a)
Indirect interaction (formation/destruction of DNA template)	NAD^+	exonuclease-assisted amplification	0.25 nM	(Wang et al. 2017a)
	coralyne	exonuclease-assisted amplification	1.83 nM	(Lee et al. 2018)
	human papillomavirus-16 DNA	ratiometric detection using two-color emitting DNA-AgNCs	5.7 pM	(Yuan et al. 2019)
	norovirus RNA	high QY (53%)	18 nM	(Shen et al. 2019)
	DNA polymerase	hairpin template	0.05 U/mL	(Kim and Gang 2019)
	mycotoxin T-2	polymerase-assisted isothermal amplification	30 fg/mL	(Zhang et al. 2019c)
	telomerase	enhancement by Mg^{2+}	2.53×10^{-9} IU	(Peng et al. 2019)
	prostate-specific antigen	simple	1.14 ng/mL	(Fang et al. 2019)
Indirect interaction (assembly on surface)	lysozyme	HCR-based amplification	42 pM	(Chen et al. 2015a)
	miRNA-21	RCA-based amplification	22 aM	(Chen et al. 2016b)
	thrombin	HCR-based amplification	0.1 fM	(Jie et al. 2017)
	methyltransferase	HCR-based amplification	0.0073 U/mL	(Peng et al. 2018)
	terminal deoxynucleotidyl transferase	graphene oxide-modified electrode	0.08 U/mL	(Hu et al. 2017)
	methyltransferase	HCR-based amplification	0.0073 U/mL	(Peng et al. 2018)
	cancer cell MCF-7	ITO (indium tin oxide) electrode platform for both imaging and electrochemical detection	3 cells	(Cao et al. 2019)
	miRNA-21	surface plasmon-enhanced ECL	0.96 aM	(Feng et al. 2019)
Imaging of cancer cell	HeLa cell	folate-linked DNA	not applicable	(Huang et al. 2018)
	breast cancer cell	high QY (87.43%)	not applicable	(Lan et al. 2019)
	breast cancer cell	quantitative analysis	3 cells	(Cao et al. 2019)
	NIH-3T3 cell	cationic polyelectrolyte modified AgNCs with enhanced emission and higher stability	not applicable	(Lyu et al. 2019)

Acknowledgement

This work was supported by the National Science Foundation of China (No. 31601552), the National Key Research and Development Program of China (No. 2017YFC1601704, 2018YFC1602300), the National First-class Discipline Program of Food Science and Technology (JUFSTR20180509) and the "Hong Kong Scholar" program.

References

Ai, J., Guo, W., Li, B., Li, T., Li, D., Wang, E., 2012. Talanta 88, 450-455.

Ardekani, L.S., Moghadam, T.T., Thulstrup, P.W., Ranjbar, B.J.P., 2019.

Bi, S., Yue, S., Zhang, S., 2017. Chem. Soc. Rev. 46(14), 4281-4298.

Bier, F.F., Scheller, F.W., 1996. Biosens. Bioelectron. 11(6), 669-674.

Borghei, Y.S., Hosseini, M., Ganjali, M.R., Hosseinkhani, S., 2018. J. Pharm. Biomed. Anal. 152, 81-88.

Cao, Y., Dai, Y., Chen, H., Tang, Y., Chen, X., Wang, Y., Zhao, J., Zhu, X., 2019. Biosens. Bioelectron. 130, 132-138.

Cao, Y., Guo, J., Shi, R., Waterhouse, G.I.N., Pan, J., Du, Z., Yao, Q., Wu, L.Z., Tung, C.H., Xie, J., Zhang, T., 2018. Nat. Commun. 9(1), 2379.

Cerretani, C., Kanazawa, H., Vosch, T., Kondo, J., 2019. Angew. Chem. Int. Ed. Engl. 0(ja).

Chen, A., Ma, S., Zhuo, Y., Chai, Y., Yuan, R., 2016a. Anal. Chem. 88(6), 3203-3210.

Chen, A., Ma, S., Zhuo, Y., Chai, Y., Yuan, R., 2016b. Anal. Chem. 88(6), 3203-3210.

Chen, L., Sha, L., Qiu, Y., Wang, G., Jiang, H., Zhang, X., 2015a. Nanoscale 7(7), 3300-3308.

Chen, Y.-A., Obliosca, J.M., Liu, Y.-L., Liu, C., Gwozdz, M.L., Yeh, H.-C., 2015b. J. Am. Chem. Soc. 137(33), 10476-10479.

Chen, Y., Phipps, M.L., Werner, J.H., Chakraborty, S., Martinez, J.S., 2018a. Acc. Chem. Res. 51(11), 2756-2763.

Chen, Z., Liu, Y., Xin, C., Zhao, J., Liu, S., 2018b. Biosens. Bioelectron. 113, 1-8.

Chi, B.-Z., Wang, C.-L., Wang, Z.-Q., Pi, T., Zhong, X.-L., Deng, C.-Q., Feng, Y.-C., Li, Z.-M., 2019. Microchim. Acta 186(4), 241.

Díez, I., Pusa, M., Kulmala, S., Jiang, H., Walther, A., Goldmann, A.S., Müller, A.H.E., Ikkala, O., Ras, R.H.A., 2009. Angew. Chem. Int. Ed. Engl. 48(12), 2122-2125.

Dirks, R.M., Pierce, N.A., 2004. Proc. Natl. Acad. Sci. USA 101(43), 15275-15278.

Fang, B.-Y., An, J., Liu, B., Zhao, Y.-D., 2019. Colloids and Surfaces B: Biointerfaces 175, 358-364.

Fang, W., Zhang, X., Chen, Y., Wan, L., Huang, W., Shen, A., Hu, J., 2015. Anal. Chem. 87(18), 9217-9224.

Feng, L., Huang, Z., Ren, J., Qu, X., 2012. Nucleic Acids Res. 40(16), e122.

Feng, L., Wu, L., Xing, F., Hu, L., Ren, J., Qu, X., 2017. Biosens. Bioelectron. 98, 378-385.

Feng, X., Han, T., Xiong, Y., Wang, S., Dai, T., Chen, J., Zhang, X., Wang, G., 2019. ACS Sensors 4(6), 1633-1640.

Gonzalez, J.I., Lee, T.-H., Barnes, M.D., Antoku, Y., Dickson, R.M., 2004. Phys. Rev. Lett. 93(14), 147402.

Grandjean, D., Coutiño-Gonzalez, E., Cuong, N.T., Fron, E., Baekelant, W., Aghakhani, S., Schlexer, P., D'Acapito, F., Banerjee, D., Roeffaers, M.B.J., Nguyen, M.T., Hofkens, J., Lievens, P., 2018. 361(6403), 686-690.

Guo, Y., Shen, F., Cheng, Y., Xie, Y., Yu, H., Yao, W., Li, H.W., Qian, H., Pei, R., 2018. Nanoscale 10(24),

11517-11523.

Guo, Y., Xu, L., Hong, S., Sun, Q., Yao, W., Pei, R., 2016. Analyst 141(24), 6481-6489.

Guo, Y., Zhang, Y., Pei, R., Cheng, Y., Xie, Y., Yu, H., Yao, W., Li, H.-W., Qian, H., 2019. Sensors and Actuators B: Chemical 281, 493-498.

Han, S., Zhu, S., Liu, Z., Hu, L., Parveen, S., Xu, G., 2012. Biosens. Bioelectron. 36(1), 267-270.

Han, Y., Zhang, F., Gong, H., Cai, C., 2019. Anal. Chim. Acta 1053, 105-113.

Hu, L., Xu, G., 2010. Chem. Soc. Rev. 39(8), 3275-3304.

Hu, Y., Zhang, Q., Guo, Z., Wang, S., Du, C., Zhai, C., 2017. Biosens. Bioelectron. 98, 91-99.

Huang, D.-J., Wu, Z., Yu, R.-Q., Jiang, J.-H., 2018. Talanta 190, 429-435.

Jeong, S., Kwon, W.Y., Hwang, S.H., Shin, J., Kim, Y., Lee, M., Park, K.S., 2019. Artif Cells Nanomed Biotechnol 47(1), 621-625.

Jia, C., Shang, J., Wang, Y., Bai, L., Tong, C., Chen, Y., Zhang, P.J.S., Chemical, A.B., 2018. 269, S0925400518308323.

Jiang, Y., Ma, X., Shao, X., Wang, M., Jiang, Y., Miao, P., 2019a. Sensors and Actuators B: Chemical 297, 126788.

Jiang, Y., Tang, Y., Miao, P., 2019b. Nanoscale 11(17), 8119-8123.

Jie, G., Tan, L., Zhao, Y., Wang, X., 2017. Biosens. Bioelectron. 94, 243-249.

Jonsson, U., Fagerstam, L., Ivarsson, B., Johnsson, B., Karlsson, R., Lundh, K., Lofas, S., Persson, B., Roos, H., Ronnberg, I., et al., 1991. BioTechniques 11(5), 620-627.

Kim, S., Gang, J., 2019. J. Nanosci. Nanotechnol. 19(10), 6534-6538.

Kong, L., Xu, J., Xu, Y., Xiang, Y., Yuan, R., Chai, Y., 2013. Biosens. Bioelectron. 42, 193-197.

Lan, J., Wu, X., Luo, L., Liu, J., Yang, L., Wang, F., 2019. Talanta 197, 86-91.

Lee, C.-Y., Lin, S.-W., Wu, Y.-H., Hsieh, Y.-Z., 2018. Anal. Chim. Acta 1042, 86-92.

Lee, S.T., Rahman, R., Muthoosamy, K., Mohamed, N.A.H., Su, X., Tayyab, S., New, S.Y., 2019. Microchim. Acta 186(2), 81.

Lequin, R.M., 2005. Clin. Chem. 51(12), 2415.

Li, B., Chen, Y., Wang, J., Lu, Q., Zhu, W., Luo, J., Hong, J., Zhou, X., 2019a. Anal. Chim. Acta 1048, 168-177.

Li, D., Qiao, Z., Yu, Y., Tang, J., He, X., Shi, H., Ye, X., Lei, Y., Wang, K., 2018. Chem. Commun. 54(9), 1089-1092.

Li, J., Ma, J., Zhang, Y., Zhang, Z., He, G., 2019b. Microchim. Acta 186(1), 48.

Li, J., Zhong, X., Zhang, H., Le, X.C., Zhu, J.-J., 2012. Anal. Chem. 84(12), 5170-5174.

Lin, C., Chen, Y., Cai, Z., Zhu, Z., Jiang, Y., Yang, C.J., Chen, X., 2015. Biosens. Bioelectron. 63, 562-565.

Lin, X., Xiao, F., Li, X., Li, F., Liu, C., Xiao, X., Hu, N., Yang, S., 2019. Microchim. Acta 186(8), 519.

Liu, J., 2014. TrAC, Trends Anal. Chem. 58, 99-111.

Liu, J., Lu, Y., Feng, L., Wang, S., Zhang, S., Zhu, X., Sheng, L., Zhang, S., Zhang, X., 2017. Anal. Chem. 89(4), 2622-2627.

Liu, S., Pang, S., 2018. Microchim. Acta 185(9), 426.

Liu, Z., Qi, W., Xu, G., 2015. Chem. Soc. Rev. 44(10), 3117-3142.

Liu, Z., Wang, Y., Li, J., Yuan, Y., Wu, X., Liu, W., Liu, Y., 2019. Anal. Chim. Acta 1087, 86-92.

Lu, S., Wang, S., Zhao, J., Sun, J., Yang, X., 2018. ACS Sensors 3(11), 2438-2445.

Lyu, D., Li, J., Wang, X., Guo, W., Wang, E., 2019. Anal. Chem. 91(3), 2050-2057.

Ma, C., Liu, H., Wu, K., Chen, M., He, H., Wang, K., Xia, K., 2018. New J. Chem. 42(6), 4331-4336.

Ma, H., Xue, N., Wu, S., Li, Z., Miao, X., 2019. Microchim. Acta 186(5), 317.

Mao, A., Wei, C., 2019. Microchim. Acta 186(8), 541.

Miao, X., Cheng, Z., Ma, H., Li, Z., Xue, N., Wang, P., 2018. Anal. Chem. 90(2), 1098-1103.

Notomi, T., Okayama, H., Masubuchi, H., Yonekawa, T., Watanabe, K., Amino, N., Hase, T., 2000. Nucleic Acids Res. 28(12), E63.

Ono, A., Cao, S., Togashi, H., Tashiro, M., Fujimoto, T., Machinami, T., Oda, S., Miyake, Y., Okamoto, I., Tanaka, Y., 2008. Chem. Commun. (39), 4825-4827.

Pan, M., Liang, M., Sun, J., Liu, X., Wang, F., 2018. Langmuir. 34(49), 14851-14857.

Peng, M., Na, N., Ouyang, J., 2019. Chemistry 25(14), 3598-3605.

Peng, X., Zhu, J., Wen, W., Bao, T., Zhang, X., He, H., Wang, S., 2018. Biosens. Bioelectron. 118, 174-180.

Pereira, R.L., Nascimento, I.C., Santos, A.P., Ogusuku, I.E.Y., Lameu, C., Mayer, G., Ulrich, H., 2018. Oncotarget 9(42), 26934-26953.

Qin, Y., Daniyal, M., Wang, W., Jian, Y., Yang, W., Qiu, Y., Tong, C., Wang, W., Liu, B., 2019. Sensors and Actuators B: Chemical 291, 485-492.

Qiu, Z., Liu, X., Lam, J.W.Y., Tang, B.Z., 2019. Macromol Rapid Commun 40(1), e1800568.

Richards, C.I., Choi, S., Hsiang, J.C., Antoku, Y., Vosch, T., Bongiorno, A., Tzeng, Y.L., Dickson, R.M., 2008. J. Am. Chem. Soc. 130(15), 5038-5039.

Schroeder, L.K., Goreham, V.R., Nann, T., 2019. Nanomaterials 9(8).

Service, R.F., 1996. Science 271(5251), 921-921.

Shah, P., Choi, S.W., Kim, H.J., Cho, S.K., Bhang, Y.J., Ryu, M.Y., Thulstrup, P.W., Bjerrum, M.J., Yang, S.W., 2016. Nucleic Acids Res. 44(6), e57.

Shangguan, D., Li, Y., Tang, Z., Cao, Z.C., Chen, H.W., Mallikaratchy, P., Sefah, K., Yang, C.J., Tan, W., 2006. Proc. Natl. Acad. Sci. USA 103(32), 11838-11843.

Shen, F., Cheng, Y., Xie, Y., Yu, H., Yao, W., Li, H.-W., Guo, Y., Qian, H., 2019. Anal. Biochem. 583, 113365.

Su, X., Chew, F.T., Li, S.F.Y., 2000. Biosens. Bioelectron. 15(11), 629-639.

Sun, Y., Hong, S., Xie, R., Huang, R., Lei, R., Cheng, B., Sun, D.E., Du, Y., Nycholat, C.M., Paulson, J.C., Chen, X., 2018. J. Am. Chem. Soc. 140(10), 3592-3602.

Tao, G., Chen, Y., Lin, R., Zhou, J., Pei, X., Liu, F., Li, N.J.N.R., 2018. 11(4), 2237-2247.

Tyagi, S., Kramer, F.R., 1996. Nat. Biotechnol. 14(3), 303-308.

Wang, C., Xing, K., Zhang, G., Yuan, M., Xu, S., Liu, D., Chen, W., Peng, J., Hu, S., Lai, W.-H., 2019a. Food Chem. 281, 91-96.

Wang, G.-L., Xu, J.-J., Chen, H.-Y., Fu, S.-Z., 2009. Biosens. Bioelectron. 25(4), 791-796.

Wang, H.Y., Ma, J.L., Yin, B.C., Ye, B.C., 2017a. Analyst 142(10), 1765-1771.

Wang, J., Gao, T., Luo, Y., Wang, Z., Zhang, Y., Zhang, Y., Zhang, Y., Pei, R., 2019b. J. Mol. Evol. 87(2-3), 72-82.

Wang, J., Li, B., Lu, Q., Li, X., Weng, C., Yan, X., Hong, J., Zhou, X., 2019c. Microchim. Acta 186(6), 356.

Wang, J., Zhang, Y., Chen, Y., Hong, S., Sun, Y., Sun, N., Pei, R., 2017b. Talanta 175, 235-242.

Wang, R., Yan, X., Sun, J., Wang, X., Zhao, X.-E., Liu, W., Zhu, S., 2018a. Anal. Methods 10(34), 4183-4188.

Wang, S., Lu, S., Zhao, J., Yang, X., 2019d. ACS Appl. Mater. Interfaces 11(28), 25066-25073.

Wang, W., Li, J., Fan, J., Ning, W., Liu, B., Tong, C., 2018b. Sensors and Actuators B: Chemical 267, 174-180.

Wu, G., Datar, R.H., Hansen, K.M., Thundat, T., Cote, R.J., Majumdar, A., 2001. Nat. Biotechnol. 19(9), 856-860.

Wu, J., Li, N., Yao, Y., Tang, D., Yang, D., Ong'achwa Machuki, J., Li, J., Yu, Y., Gao, F., 2018. Anal. Chem. 90(24), 14368-14375.

Xu, H., Yu, L., Zhang, S., Xu, X., Chen, T., Ye, H., Zhu, X., 2019. Luminescence : the journal of biological and chemical luminescence 0(0).

Xu, J., Wei, C., 2017. Biosens. Bioelectron. 87, 422-427.

Xu, M., Gao, Z., Wei, Q., Chen, G., Tang, D., 2016. Biosens. Bioelectron. 79, 411-415.

Yan, X., Sun, J., Zhao, X.-E., Wang, R., Wang, X., Zuo, Y.-N., Liu, W., Kong, R., Zhu, S.J.M.A., 2018. Microchim. Acta 185(9), 403.

Yang, C., Shi, K., Dou, B., Xiang, Y., Chai, Y., Yuan, R., 2015. ACS Appl. Mater. Interfaces 7(2), 1188-1193.

Yang, S.W., Vosch, T., 2011. Anal. Chem. 83(18), 6935-6939.

Yang, X., Sun, J.-K., Kitta, M., Pang, H., Xu, Q., 2018. Nature Catalysis 1(3), 214-220.

Yao, Q., Chen, T., Yuan, X., Xie, J., 2018. Acc. Chem. Res. 51(6), 1338-1348.

Yao, Y., Li, N., Zhang, X., Ong'achwa Machuki, J., Yang, D., Yu, Y., Li, J., Tang, D., Tian, J., Gao, F., 2019. ACS Appl. Mater. Interfaces 11(15), 13991-14003.

Ye, T., Chen, J., Liu, Y., Ji, X., Zhou, G., He, Z., 2014. ACS Appl. Mater. Interfaces 6(18), 16091-16096.

Ye, T., Peng, Y., Yuan, M., Cao, H., Yu, J., Li, Y., Xu, F., 2018. Microchim. Acta 186(1), 40.

Yeh, H.-C., Sharma, J., Shih, I.-M., Vu, D.M., Martinez, J.S., Werner, J.H., 2012. J. Am. Chem. Soc. 134(28), 11550-11558.

Yeh, H.C., Sharma, J., Han, J.J., Martinez, J.S., Werner, J.H., 2010. Nano Lett. 10(8), 3106-3110.

Yi, J., Liu, Z., Liu, J., Liu, H., Xia, F., Tian, D., Zhou, C., 2020. Biosens. Bioelectron. 148, 111827.

Yuan, Y., Ma, Y., Luo, L., Wang, Q., Huang, J., Liu, J., Yang, X., Wang, K., 2019. Microchim. Acta 186(9), 613.

Zhang, C., Gao, D., Zhou, G., Chen, L., Zhang, X.A., Cui, Z., He, Z., 2012a. Chem. Asian. J. 7(8), 1764-1767.

Zhang, J., Liu, Y., Zhi, X., Zhang, C., Liu, T.F., Cui, D., 2018a. Nanoscale 10(23), 11079-11090.

Zhang, K., Huang, W., Huang, Y., Wang, K., Zhu, X., Xie, M., 2019a. Microchim. Acta 186(3), 181.

Zhang, M., Gao, G., Ding, Y., Deng, C., Xiang, J., Wu, H., 2019b. Talanta 199, 238-243.

Zhang, M., Guo, S.M., Li, Y.R., Zuo, P., Ye, B.C., 2012b. Chem. Commun. 48(44), 5488-5490.

Zhang, M., Wang, Y., Yuan, S., Sun, X., Huo, B., Bai, J., Peng, Y., Ning, B., Liu, B., Gao, Z., 2019c. Microchim. Acta 186(4), 219.

Zhang, P., Jia, C., Zhao, Y., Luo, H., Tan, X., Ma, X., Wang, Y., 2019d. Microchim. Acta 186(9), 609.

Zhang, S., Wang, K., Li, K.B., Shi, W., Jia, W.P., Chen, X., Sun, T., Han, D.M., 2017. Biosens. Bioelectron. 91, 374-379.

Zhang, X., Chen, F., Song, X., He, P., Zhang, S., 2018b. Biosens. Bioelectron. 104, 27-31.

Zhang, X.D., Luo, Z., Chen, J., Shen, X., Song, S., Sun, Y., Fan, S., Fan, F., Leong, D.T., Xie, J., 2014. Adv. Mater. 26(26), 4565-4568.

Zhang, Y., Zhu, C., Zhang, L., Tan, C., Yang, J., Chen, B., Wang, L., Zhang, H., 2015. Small 11(12), 1385-1389.

Zhao, W., Liu, M., Li, H., Wang, S., Tang, S., Kong, R.M., Yu, R., 2019. Biosens. Bioelectron. 143, 111593.

Zhong, W., Pu, Y., Tan, W., Liu, J., Liao, J., Liu, B., Chen, K., Yu, B., Hu, Y., Deng, Y., Zhang, J., Liu, H., 2019. Anal. Chem. 91(13), 8289-8297.

Zhou, W., Zhu, J., Teng, Y., Du, B., Han, X., Dong, S., 2018. Nano Research 11(4), 2012-2023.

Zhou, Z., Du, Y., Dong, S., 2011. Biosens. Bioelectron. 28(1), 33-37.

Zhu, G., Ye, M., Donovan, M.J., Song, E., Zhao, Z., Tan, W., 2012. Chem. Commun. 48(85), 10472-10480.

Zhu, R., Luo, X., Deng, L., Lei, C., Huang, Y., Nie, Z., Yao, S., 2018. Analyst 143(12), 2908-2914.

Zhu, Y.-J., Li, W.-J., Hong, Z.-Y., Tang, A.-N., Kong, D.-M., 2017. J. Mater. Chem. B 5(46), 9229-9237.

1. DNA-AgNCs have demonstrated pervasive applications and attracted interests in biosensors development recently.

2. Most of the recently reported label-free probes based on DNA-AgNCs signal output were classified legitimately.

3. The design principles of each kind of probe were explained thoroughly to help readers better understand and apply such strategies.

4. Besides the discussion and perspective in the last part, a short summary was made for each section.

This manuscript was proposed by Dr. Guo to start writing. In the whole process of writing, Professor Li gave full guidance; Miss Pan, Miss Zhang and Dr. Wong helped in literature collection and language touch-up; Dr. Hu and Professor He gave support in content setting, manuscript review and editing. The authors declare no conflict of interest. The specific contributions are as follows:

Yahui Guo, writing original manuscript;

Xinyue Pan, collecting references;

Wenya Zhang, classification of references;

Zhigang Hu, discuss and analyzing references;

Ka-Wang Wong, review and editing mainly for linguistic quality;

Zhike He, review and editing for the whole content of this manuscript;

Hung-Wing Li, supervision and funding acquisition.

Declaration of interests

☒ The authors declare that they have no known competing financial interests or personal relationships that could have appeared to influence the work reported in this paper.

☐The authors declare the following financial interests/personal relationships which may be considered as potential competing interests: